POLITECNICO DI TORINO
Repository ISTITUZIONALE

SEISMIC PERFORMANCE OF BRIDGES EQUIPPED WITH FPS

(Article begins on next page)

19 April 2024

PRESTAZIONE SISMICA DI PONTI DOTATI DI ISOLATORI FPS

SEISMIC PERFORMANCE OF BRIDGES EQUIPPED WITH FPS

Paolo Castaldo,
Elena Miceli,
Diego Gino,
Guglielmo Amendola,
Luca Giordano

Politecnico di Torino
Department of Structural, Geotechnical and Building Engineering (DISEG)
Turin, Italy
paolo.castaldo@polito.it; elena.miceli@polito.it; diego.gino@polito.it; gugliel-mo.amendola@polito.it; luca.giordano@polito.it

ABSTRACT

The scope of the present study is focused on the evaluation of the seismic response of bridges isolated by single concave sliding pendulum isolators (FPS) for the different structural properties when the presence of the rigid abutment is considered or neglected (i.e., isolated viaducts). In this way, they have been defined two specific multi-degree-of-freedom (mdof) models to simulate the elastic behavior of the reinforced concrete pier in combination to the infinitely rigid presence of the deck and to the presence of the rigid abutment if considered. Both the numerical models also account for the non-linear velocity-dependent behavior of the FPS bearings. Considering the aleatory uncertainty in the seismic input by means of several natural records with different characteristics, a parametric analysis is developed for several structural properties. The relevant results expressed as the statistics in non-dimensional form with respect to the seismic intensity have permitted to study the differences between the two numerical models in relation to the effectiveness of the seismic isolation.

SOMMARIO

Lo scopo del presente studio è focalizzato sulla valutazione della risposta sismica di ponti isolati da con dispositivi a pendolo scorrevole (FPS) per diverse proprietà strutturali considerando o tra-

scurando la presenza rigida della spalla. In questo modo sono stati definiti due specifici modelli a più gradi di libertà per simulare il comportamento elastico della pila in combinazione alla presenza infinitamente rigida dell'impalcato e alla presenza rigida della spalla se considerata. Entrambi i modelli numerici tengono conto anche del comportamento non lineare dipendente dalla velocità dei dispositivi FPS. Considerando l'incertezza aleatoria nell'input sismico per mezzo di più registrazioni accelerometriche naturali con caratteristiche differenti, viene sviluppata un'analisi parametrica al variare delle proprietà strutturali. I risultati rilevanti espressi come statistiche in forma adimensionale rispetto all'intensità sismica hanno permesso di studiare le differenze tra i due modelli numerici in relazione all'efficacia dell'isolamento sismico.

1   INTRODUCTION

The goal of seismic isolation of bridges is to reduce the forces transmitted from the deck to the substructure, i.e., the piers, by increasing the period of the isolation system. During the past years, both the elastomeric and frictional isolators have demonstrated their effectiveness in enhancing seismic performance of structures and infrastructures [1]-[3]. In this context, an isolated three-span continuous deck bridge, equipped with elastomeric bearings, is studied in [4], with the goal to evaluate the bearings peak displacement placed at abutment locations. On the other hand, among the widely adopted isolators, the friction pendulum system (FPS) bearings have the advantage of making the properties of the device independent from the mass deck, which is important in the design phase of the isolator [5]. In particular, the introduction of the optimal friction coefficient, able to minimize the seismic response of the pier, was first introduced by Jangid in [6]. In this respect, the optimal friction coefficient is studied in [7] by varying many properties of the structure and the seismic input.

The goal of this work is to evaluate the pier-abutment-deck interaction when bridges are equipped with single concave friction pendulum isolators (FPS). In particular, two six-degree-of-freedom (dofs) models are compared: one representative of a single column bent viaduct (i.e., neglecting the presence of the rigid abutment) and the other for the case of multi-span continuous deck bridge (i.e., including the presence of the abutment). More precisely, for both cases, five dofs are adopted for the lumped masses of the elastic pier and one additional dof representative of the infinitely rigid deck. The equations of motion under a set of seismic inputs are solved for both the models, by performing a non-dimensional analysis. The FPS behaviour is represented by a widespread model that includes the dependency of the friction coefficient from the velocity. Many bridge properties are varied so as to perform a parametric analysis. Then, after having obtained the peak non-dimensional response at the pier level, the optimal sliding friction coefficient, able at minimizing this response, is investigated.

2   NON DIMENSIONAL ANALYSIS AND PROBLEM PARAMETERS

To model the seismic response of bridges, both including or neglecting the presence of the rigid abutment, a six-degree-of-freedom (dofs) model is adopted, where 5 dofs are used for the lumped masses of the reinforced concrete (RC) elastic pier, as suggested in [8], and 1 additional dof is for the infinitely rigid RC deck.

Focusing on the case of multi-span continuous deck bridge, where the rigid RC abutment is modelled (Fig. 1), subjected to a seismic input along the longitudinal direction, the equation of motion are:

$$
\begin{bmatrix}
m_d & m_d & m_d & m_d & m_d & m_d \\
0 & m_{p5} & m_{p5} & m_{p5} & m_{p5} & m_{p5} \\
0 & 0 & m_{p4} & m_{p4} & m_{p4} & m_{p4} \\
0 & 0 & 0 & m_{p3} & m_{p3} & m_{p3} \\
0 & 0 & 0 & 0 & m_{p2} & m_{p2} \\
0 & 0 & 0 & 0 & 0 & m_{p1}
\end{bmatrix}
\begin{bmatrix}
\ddot{u}_d(t) \\
\ddot{u}_{p5}(t) \\
\ddot{u}_{p4}(t) \\
\ddot{u}_{p3}(t) \\
\ddot{u}_{p2}(t) \\
\ddot{u}_{p1}(t)
\end{bmatrix}
+
\begin{bmatrix}
c_d & 0 & 0 & 0 & 0 & 0 \\
-c_d & c_{p5} & 0 & 0 & 0 & 0 \\
0 & -c_{p5} & c_{p4} & 0 & 0 & 0 \\
0 & 0 & -c_{p4} & c_{p3} & 0 & 0 \\
0 & 0 & 0 & -c_{p3} & c_{p2} & 0 \\
0 & 0 & 0 & 0 & -c_{p2} & c_{p1}
\end{bmatrix}
\begin{bmatrix}
\dot{u}_d(t) \\
\dot{u}_{p5}(t) \\
\dot{u}_{p4}(t) \\
\dot{u}_{p3}(t) \\
\dot{u}_{p2}(t) \\
\dot{u}_{p1}(t)
\end{bmatrix}
+
$$

$$
+
\begin{bmatrix}
\frac{m_d}{2}g/R_p+\frac{m_d}{2}g/R_a & \frac{m_d}{2}g/R_a & \frac{m_d}{2}g/R_a & \frac{m_d}{2}g/R_a & \frac{m_d}{2}g/R_a & \frac{m_d}{2}g/R_a \\
-\frac{m_d}{2}g/R_p & k_{p5} & 0 & 0 & 0 & 0 \\
0 & -k_{p5} & k_{p4} & 0 & 0 & 0 \\
0 & 0 & -k_{p4} & k_{p3} & 0 & 0 \\
0 & 0 & 0 & -k_{p3} & k_{p2} & 0 \\
0 & 0 & 0 & 0 & -k_{p2} & k_{p1}
\end{bmatrix}
\begin{bmatrix}
u_d \\
u_{p5} \\
u_{p4} \\
u_{p3} \\
u_{p2} \\
u_{p1}
\end{bmatrix}
+
\tag{1}
$$

$$
+
\begin{bmatrix}
\frac{m_d}{2}g\mu_p(\dot{u}_d(t))Z(t)+\frac{m_d}{2}g\mu_a\left(\dot{u}_d(t)+\sum_{i=1}^{5}\dot{u}_{pi}(t)\right)Z(t) \\
-\frac{m_d}{2}g\mu_p(\dot{u}_d(t))Z(t) \\
0 \\
0 \\
0 \\
0
\end{bmatrix}
=+\ddot{u}_g(t)\cdot
\begin{bmatrix}
-m_d \\
-m_{p5} \\
-m_{p4} \\
-m_{p3} \\
-m_{p2} \\
-m_{p1}
\end{bmatrix}
$$

where u_d is the deck displacement with respect to the pier top, u_{pi} is the displacement of the ith lumped mass of the pier with respect to the lower one, m_d is the mass of the deck, m_{pi} is the mass of the ith lumped mass of the pier, k_{pi} is the corresponding stiffness, c_d and c_{pi} are, respectively, the viscous damping coefficient for the device and for the pier masses, $Z(t)$ indicate the sign function of the velocity, with t the instant of time and the dots indicate differentiation. The resisting forces of the FPS bearings located on top of the abutment and on the pier are, respectively, $F_a(t)$ and $F_p(t)$, expressed as the sum of an elastic component and a viscous component [9]:

$$
F_a(t)=\frac{m_d g}{2}\left[\frac{1}{R_a}\left(u_d(t)+\sum_{i=1}^{5}u_{pi}\right)+\mu_a\left(\dot{u}_d+\sum_{i=1}^{5}\dot{u}_{pi}\right)\mathrm{sgn}\left(\dot{u}_d+\sum_{i=1}^{5}\dot{u}_{pi}\right)\right]
$$

$$
F_p(t)=\frac{m_d g}{2}\left[\frac{1}{R_p}u_d(t)+\mu_p(\dot{u}_d)\mathrm{sgn}(\dot{u}_d)\right]
\tag{2}
$$

where the stiffness of the deck is equal to $k_d=W/R=m_d g/R$, half for the bearing on the abutment and half for the pier, the radii of curvature of the FPS bearings are R_a and R_p, placed, respectively, on the abutment and on the pier and assumed equal, g is the gravity constant, μ is the sliding friction coefficient of the bearings. As anticipated, the fundamental period of the deck only depends on the geometrical properties of the isolator, since it is expressed as $T_d=2\pi\sqrt{m_d/k_d}=2\pi\sqrt{R/g}$ [9]. It noteworthy that the two expressions in (2) differ only in terms of displacements, since $F_a(t)$ depends on the relative displacement of the deck with respect to the ground while $F_p(t)$ is function of the deck displacement with respect to the pier top. Regarding the sliding friction coefficient, its dependency on the velocity is such that [10]:

$$\mu(\dot{u}_d) = f_{\max} - (f_{\max} - f_{\min}) \cdot \exp(-\alpha|\dot{u}_d|) \tag{3}$$

where $f_{\max}$ and $f_{\min}$ are the sliding friction parameters at maximum and zero velocity, α is a parameter that controls the transition from low to large velocities. In this work, it is assumed α equal to 30 and $f_{\max} = 3f_{\min}$.

The equation of motions expressed in (1) are then elaborated so as to obtain their nondimensional form, according to the Buckingham's Π-theorem [11]. In particular, a time scale is introduced and assumed equal to $1/\omega_d$, with $\omega_d = \sqrt{k_d/m_d}$ indicating the circular frequency of the isolation system. Thus, passing from the time t to $\tau = t\omega_d$, the ground motion input of equation (1) becomes $\ddot{u}_g(t) = a_0 l(t) = a_0 \ell(\tau)$, where $l(t)$ is a nondimensional function of the seismic input time-history over time t, while $\ell(\tau)$ contains the same information in the new time τ. In addition, a length scale is introduced equal to a_0/ω_d^2, where a_0 is an intensity measure for the seismic input. In the end, dividing the equations in (1) for the deck mass m_d and introducing the time and length scales, the nondimensional equations become:

$$
\begin{bmatrix}
1 & 1 & 1 & 1 & 1 & 1 \\
0 & \lambda_{p5} & \lambda_{p5} & \lambda_{p5} & \lambda_{p5} & \lambda_{p5} \\
0 & 0 & \lambda_{p4} & \lambda_{p4} & \lambda_{p4} & \lambda_{p4} \\
0 & 0 & 0 & \lambda_{p3} & \lambda_{p3} & \lambda_{p3} \\
0 & 0 & 0 & 0 & \lambda_{p2} & \lambda_{p2} \\
0 & 0 & 0 & 0 & 0 & \lambda_{p1}
\end{bmatrix}
\begin{bmatrix}
\ddot{\psi}_d(\tau) \\
\ddot{\psi}_{p5}(\tau) \\
\ddot{\psi}_{p4}(\tau) \\
\ddot{\psi}_{p3}(\tau) \\
\ddot{\psi}_{p2}(\tau) \\
\ddot{\psi}_{p1}(\tau)
\end{bmatrix} +
$$

$$
+\begin{bmatrix}
2\xi_d & 0 & 0 & 0 & 0 & 0 \\
-2\xi_d & 2\xi_{p5}\dfrac{\omega_{p5}}{\omega_d}\lambda_{p5} & 0 & 0 & 0 & 0 \\
0 & -2\xi_{p5}\dfrac{\omega_{p5}}{\omega_d}\lambda_{p5} & 2\xi_{p4}\dfrac{\omega_{p4}}{\omega_d}\lambda_{p4} & 0 & 0 & 0 \\
0 & 0 & -2\xi_{p4}\dfrac{\omega_{p4}}{\omega_d}\lambda_{p4} & 2\xi_{p3}\dfrac{\omega_{p3}}{\omega_d}\lambda_{p3} & 0 & 0 \\
0 & 0 & 0 & -2\xi_{p3}\dfrac{\omega_{p3}}{\omega_d}\lambda_{p3} & 2\xi_{p2}\dfrac{\omega_{p2}}{\omega_d}\lambda_{p2} & 0 \\
0 & 0 & 0 & 0 & -2\xi_{p2}\dfrac{\omega_{p2}}{\omega_d}\lambda_{p2} & 2\xi_{p1}\dfrac{\omega_{p1}}{\omega_d}\lambda_{p1}
\end{bmatrix}
\begin{bmatrix}
\dot{\psi}_d(\tau) \\
\dot{\psi}_{p5}(\tau) \\
\dot{\psi}_{p4}(\tau) \\
\dot{\psi}_{p3}(\tau) \\
\dot{\psi}_{p2}(\tau) \\
\dot{\psi}_{p1}(\tau)
\end{bmatrix} +
$$

$$
+\begin{bmatrix}
1 & 0 & 0 & 0 & 0 & 0 \\
-1 & \lambda_{p5}\dfrac{\omega_{p5}^2}{\omega_d^2} & 0 & 0 & 0 & 0 \\
0 & -\lambda_{p5}\dfrac{\omega_{p5}^2}{\omega_d^2} & \lambda_{p4}\dfrac{\omega_{p4}^2}{\omega_d^2} & 0 & 0 & 0 \\
0 & 0 & -\lambda_{p4}\dfrac{\omega_{p4}^2}{\omega_d^2} & \lambda_{p3}\dfrac{\omega_{p3}^2}{\omega_d^2} & 0 & 0 \\
0 & 0 & 0 & -\lambda_{p3}\dfrac{\omega_{p3}^2}{\omega_d^2} & \lambda_{p2}\dfrac{\omega_{p2}^2}{\omega_d^2} & 0 \\
0 & 0 & 0 & 0 & -\lambda_{p2}\dfrac{\omega_{p2}^2}{\omega_d^2} & \lambda_{p1}\dfrac{\omega_{p1}^2}{\omega_d^2}
\end{bmatrix}
\begin{bmatrix}
\psi_d(\tau) \\
\psi_{p5}(\tau) \\
\psi_{p4}(\tau) \\
\psi_{p3}(\tau) \\
\psi_{p2}(\tau) \\
\psi_{p1}(\tau)
\end{bmatrix} +
\begin{bmatrix}
\dfrac{g\mu(\dot{\psi}_d(\tau))}{a_0}\mathrm{sgn}(\dot{\psi}_d(\tau)) \\
-\dfrac{g\mu(\dot{\psi}_d(\tau))}{a_0}\mathrm{sgn}(\dot{\psi}_d(\tau)) \\
0 \\
0 \\
0 \\
0
\end{bmatrix}
= +l(\tau)\cdot
\begin{bmatrix}
-1 \\
-\lambda_{p5} \\
-\lambda_{p4} \\
-\lambda_{p3} \\
-\lambda_{p2} \\
-\lambda_{p1}
\end{bmatrix}
\tag{4}
$$

where $\psi_d = u_d \omega_d^2 / a_0$ and $\psi_{pi} = u_{pi} \omega_d^2 / a_0$ are the nondimensional displacements, $\omega_d = \sqrt{k_d / m_d}$ and $\omega_{pi} = \sqrt{k_{pi} / m_{pi}}$ are the circular vibration frequencies, $\xi_d = c_d / 2 m_d \omega_d$ and $\xi_{pi} = c_{pi} / 2 m_{pi} \omega_{pi}$ are the damping factors (respectively for the deck and for the i-th lamped masses of the pier) and $\lambda_p = \lambda_{pi} = m_{pi} / m_d$ is the mass ratio of the i-th lumped mass (all the lumped masses are assumed equal). Hence, the nondimensional parameters Π of the problem are:

$$\Pi_{\omega_p} = \frac{\omega_p}{\omega_d}, \quad \Pi_{\omega_g} = \frac{\omega_d}{\omega_g}, \quad \Pi_\lambda = \lambda_p, \quad \Pi_{\xi_d} = \xi_d, \quad \Pi_{\xi_p} = \xi_{pi}, \quad \Pi_\mu = \frac{\mu(\dot\psi_d)g}{a_0} \tag{5}$$

In the end, to discard the dependency of the nondimensional parameter Π_μ from the velocity, its value is substituted by $\Pi_\mu^* = f_{\max} g / a_0$. Regarding the equations of motion for the case of a single-column bent viaduct (Fig. 2), the nondimensional equation of motion are equal to the ones in (1) and (4), without the term $F_a(t)$.
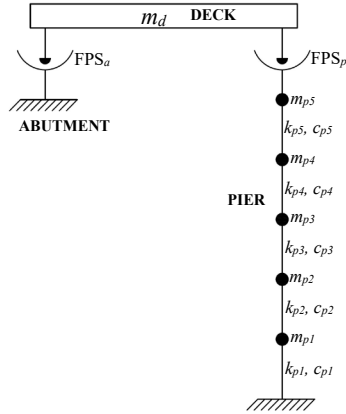

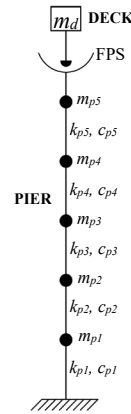**Fig. 1** Six dof model (considering the presence of the abutment)   **Fig. 2**. Six dof model (neglecting the presence of the abutment)

Regarding the main properties of the problem, the following assumptions are valid both for the case of considering or neglecting the presence of the pier-deck-abutment interaction. First of all, concerning the seismic input, a set of 30 seismic ground motions is considered, selected from 19 different earthquakes [12]-[14]. The magnitude varies in the range 6.3 to 7.5, the source-to-site distance goes from 13 km to 98 km and the peak ground acceleration is in the range 0.13 - 0.82 g. The intensity measure (IM), as also previously indicated as the seismic intensity a_0, is herein chosen as the spectral pseudo-acceleration $S_A(T_d, \xi_d)$. Assuming the damping ratio ξ_d equal to zero [15], the spectral pseudo-acceleration becomes only function of the deck fundamental period, meaning that $a_0 = S_A(T_d, \xi_d)$. Regarding the structural properties, the damping ratios are set equal to $\Pi_{\xi_d} = \xi_d = 0\%$ and $\Pi_{\xi_p} = \xi_p = 5\%$, the isolation period varies from 0.10s to 0.20s, the deck period is in the range 2s-4s, the mass ratio assumes the value 0.1, 0.15, 0.2 and, finally, the normalized friction coefficient is in between 0 and 2.

The equation of motions expressed in (4) are solved for each of the two models by varying the previously mentioned parameters and by considering each of the 30 ground motions, using the Runge-Kutta-Fehlberg integration algorithm available in Matlab-Simulink [16]. For each simulation, the peak normalised response in terms of pier top displacement is numerically calculated and expressed as:

$$\psi_{u_p} = u_{p,\max} \omega_d^2 / a_0 = \left(\sum_{i=1}^{5} u_{p_i}\right)_{\max} \omega_d^2 / a_0 \tag{6}$$

Then, the response parameters are probabilistically treated and assumed as lognormally distributed [15],[17], with geometric mean $GM\left(\psi_{u_p}\right) = \sqrt[N]{\psi_{u_p}1 \cdot \ldots \cdot \psi_{u_p}N}$, where $\psi_{u_p}j$ is the j-th realization of the response parameter and $j=1,\ldots,N$ with $N=30$ the total number of seismic inputs.

4 SEISMIC RESPONSE AND OPTIMAL FRICTION COEFFICIENT

In this section, the response of the pier and the optimal friction coefficient results are illustrated. Fig. 3 shows, for both the structural systems, the mean value of the maximum normalized pier displacement $GM\left(\psi_{u_p}\right)$ as function of T_d and Π_μ^*, for fixed values of T_p and λ. The mean value decreases for larger values of T_d and of λ. On the opposite, the response is lower for lower values of pier period.
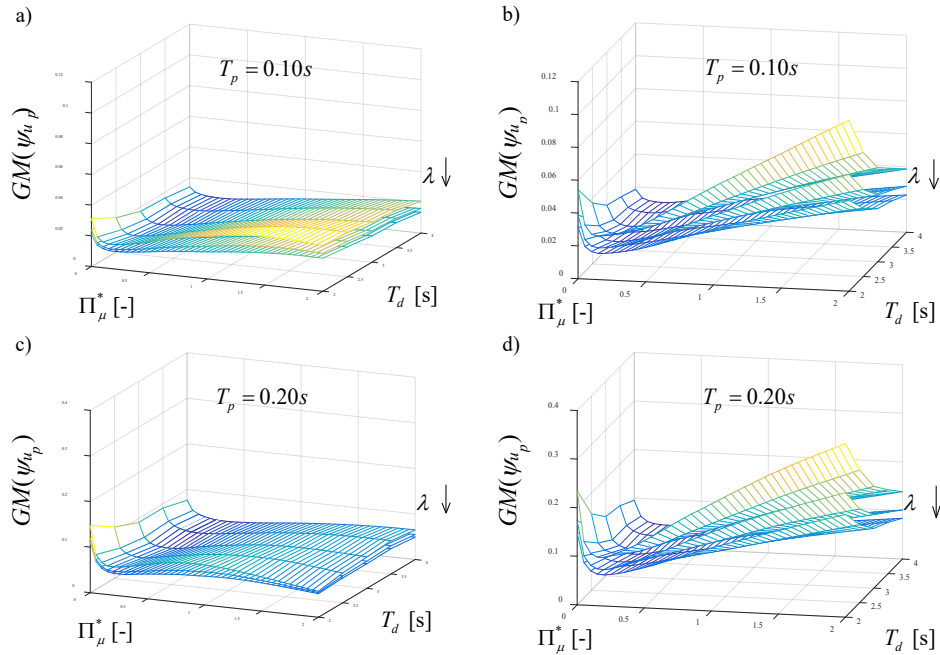

Fig. 3. 50th percentile of the maximum normalized pier displacement as function of Π^*_μ, Td and fixed values of Tp: (a)-(c) considering the abutment; (b)-(d) neglecting the abutment
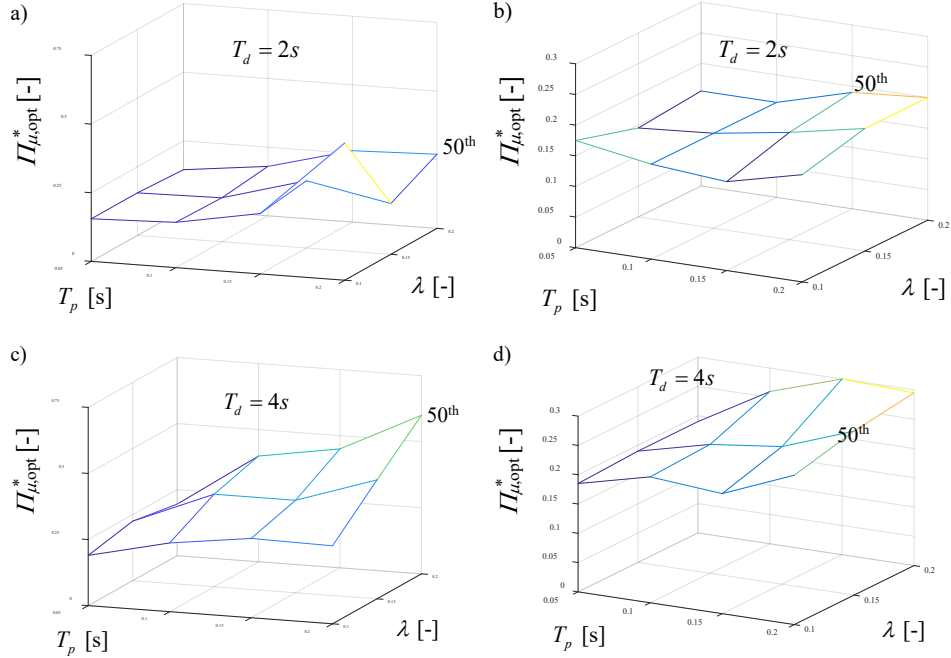
Fig. 4. Optimal friction coefficient as function of Tp and λ and for fixed values of Td: (a)-(c) considering the abutment; (b)-(d) neglecting the abutment

In addition, it is possible to observe the existence of an optimal value where the response is minimized. In fig. 4 it is illustrated the optimum of Π_μ^*, which is not only function of the parameters involved in the problem (i.e., T_d, T_p, λ), but it also depends on the structural system (i.e., if considering or not the presence of the abutment). In particular, the sagging zones of the response as function of Π_μ^* are more pronounced when the interaction with the abutment is not considered, since the bearing on top of the abutment slides faster than the device placed on the pier. Furthermore, when all the structural parameters Π_μ^*, T_p, T_d are considered with their maximum values, larger values of the optimum friction coefficient are required to increase the energy dissipation.

5   CONCLUSIONS

This work analyses the seismic performance of bridges isolated with single concave friction pendulum bearings, focusing on the pier-abutment-deck interaction. In particular, two six-degree-of-freedom structural systems are modelled: one including the presence of the abutment (i.e., multi-span continuous deck bridge) and another neglecting its presence (i.e., single-column bent viaduct). Different values for the main problem parameters are considered within a parametric analysis and the uncertainty in the seismic input is included by considering a set of 30 natural ground motions. The equations of motions are numerically solved in a non-dimensional form so as to evaluate the maximum normalized response of the pier. This response tends to first decrease and

then increase as function of the normalized friction coefficient of the bearing. When the presence of the abutment is considered (i.e., multi-span continuous deck bridge), this minimum value is less pronounced, since the bearing on top of the abutment tends to slide faster than the one on the pier. The existence of a minimum value for the pier response has suggested to evaluate an optimal value for the normalized friction coefficient, as function of the other parameters involved. In the case multi-span continuous deck bridge, higher optimal values are observed.

REFERENCES

[1] Constantinou M. C., Kartoum A., Reinhorn A. M., Bradford P., Sliding isolation system for bridges: Experimental study, Earthquake Spectra 8(3): 321-344, 1992

[2] Kartoum A., Constantinou M. C., Reinhorn A. M., Sliding isolation system for bridges: Analytical study, Journal of Structural Engineering 8(3): 345-372, 1992

[3] Jangid R. S., Equivalent linear stochastic seismic response of isolated bridges, Journal of Sound and Vibration 309(3-5): 805-822, 2008

[4] Tongaonkar N. P., Jangid R. S., Seismic response of isolated bridges with soil–structure interaction, Soil Dynamics and Earthquake Engineering 23: 287–302, 2003

[5] Su L., Ahmadi G., Tadjbakhsh I. G., Comparative study of base isolation systems, Journal of Engineering Mechanic 115(9): 1976–92, 1989

[6] Jangid R. S., Optimum frictional elements in sliding isolation systems, Computers and Structures 76(5): 651–661, 2000

[7] Castaldo P., Amendola G., Optimal DCFP bearing properties and seismic performance assessment in nondimensional form for isolated bridges, Earthquake Engineering and Structural Dynamics 50(9): 2442–2461, 2021

[8] Castaldo P., Amendola G., Optimal Sliding Friction Coefficients for Isolated Viaducts and Bridges: A Comparison Study, Structural Control and Health Monitoring 28(12), 2021

[9] Zayas V., Low S., Mahin S., A simple pendulum technique for achieving seismic isolation, Earthquake Spectra 6(2): 317-333, 1990

[10] Mokha A., Constantinou M. C., Reinhorn A. M., Teflon Bearings in Base Isolation. I: Testing, Journal of Structural Engineering 116(2): 438-454, 1990

[11] Makris N., Black C.J., Dimensional analysis of inelastic structures subjected to near fault ground motions, Technical report: EERC 2003/05, Berkeley: Earthquake Engineering Research Center, University of California, 2003

[12] PEER, Pacific Earthquake Engineering Research Center http://peer.berkeley.edu/

[13] ITACA, Italian Accelerometric Archive http://itaca.mi.ingv.it/ItacaNet/itaca10_links.htm

[14] ISESD, Internet-Site for European Strong-Motion Data http://www.isesd.hi.is/ESD_Local/frameset.htm

[15] Ryan K., Chopra A., Estimation of Seismic Demands on Isolators Based on Nonlinear Analysis, Journal of Structural Engineering 130(3): 392-402, 2004

[16] Math Works Inc, MATLAB-High Performance Numeric Computation and Visualization Software. User's Guide. Natick (MA), USA, 1997

[17] Castaldo P., Ripani M., Optimal design of friction pendulum system properties for isolated structures considering different soil conditions, Soil Dynamics and Earthquake Engineering 90: 74–87, 2016

KEYWORDS

seismic isolation, friction pendulum isolators, isolated bridges, non-dimensional form